Rate constants, branching fractions, and energy disposal for the H+ClO and H+SF reactions

S. J. Wategaonkar and D. W. Setser

Citation: The Journal of Chemical Physics **90**, 6223 (1989); doi: 10.1063/1.456339
View online: http://dx.doi.org/10.1063/1.456339
View Table of Contents: http://scitation.aip.org/content/aip/journal/jcp/90/11?ver=pdfcov
Published by the AIP Publishing

Rate constants, branching fractions, and energy disposal for the H+ClO and H+SF reactions

S. J. Wategaonkar and D. W. Setser
Department of Chemistry, Kansas State University, Manhattan, Kansas 66506

(Received 1 November 1988; accepted 9 February 1989)

The H + ClO and SF reactions have been isolated and studied by infrared chemiluminescence in a fast flow reactor. The OH product channel is favored over the HCl channel by a factor of 4.5 and the total rate constant is $(7.7 \pm 1.9) \times 10^{-11}$ cm^3 s^{-1} for the H + ClO reaction. Both sets of products are accessed from a bound singlet intermediate with HCl + O(^3P) formed by a singlet–triplet surface crossing in the exit channel; the energy disposal is $\langle f_V(\mathrm{OH}) \rangle = 0.45$ and $\langle f_V(\mathrm{HCl}) \rangle = 0.31$. The H + SF reaction gives only HF + S(^3P), but the energy disposal differs dramatically from the HCl channel of the ClO reaction. This difference arises from changes in the thermochemistry, which result in an earlier crossing to the HSF triplet surface followed by release of repulsive energy as the HF separates from the S(^3P) atom.

I. INTRODUCTION

Our attempt to study the H + ClO reaction as a secondary step in the H + Cl_2O/ClO_2 reaction systems was described in a previous paper.[1] The nascent vibrational distributions for OH and HCl were estimated using the infrared chemiluminescence (IRCL) method. However, the high $\{H + H_2\}$ concentration required in those experiments prevented reliable assignment of the branching ratio and the total rate constant. In this work the ClO and SF radicals were generated in a prereactor and then added to a flow of H atoms in a fast flow reactor. The OH, HCl, and HF products were observed by IRCL. The objectives were to improve our understanding of the ClO reaction, and to develop the prereactor method for studying atom–radical reactions. The thermochemistry[2,3] of the exit channels is given below:

$$\mathrm{H + ClO \rightarrow OH + Cl;} \qquad \Delta H^\circ_0 = -36.7 \text{ kcal mol}^{-1}, \tag{1a}$$

$$\rightarrow \mathrm{Cl + O(^3}P\mathrm{);} \qquad \Delta H^\circ_0 = -37.7 \text{ kcal mol}^{-1}, \tag{1b}$$

$$\rightarrow \mathrm{HCl + O(^1}D\mathrm{);} \qquad \Delta H^\circ_0 = +7.7 \text{ kcal mol}^{-1}, \tag{1c}$$

$$\mathrm{H + SF \rightarrow HF + S(^3}P\mathrm{);} \qquad \Delta H^\circ_0 = -54.1 \text{ kcal mol}^{-1}, \tag{2a}$$

$$\rightarrow \mathrm{HF + S(^1}D\mathrm{);} \qquad \Delta H^\circ_0 = -27.7 \text{ kcal mol}^{-1}, \tag{2b}$$

$$\rightarrow \mathrm{HS + F;} \qquad \Delta H^\circ_0 = -3.4 \text{ kcal mol}^{-1}. \tag{2c}$$

The ClO radicals were prepared using reaction (3), which has a rate constant[4] of 5.9×10^{-11} cm^3 s^{-1}. This reaction provides a clean source of ClO radicals

$$\mathrm{Cl + ClO_2 \rightarrow 2\ ClO.} \tag{3}$$

The reactions between ClO radicals and Cl, Cl_2, and ClO_2 are endoergic and need not be considered, only the disproportionation reaction removes ClO radicals. Fortunately, the rate constant[5] for disproportionation is small, $\leqslant 1.0 \times 10^{-14}$ cm^3 s^{-1}, and reaction (3) proceeds stoichiometrically to give $[\mathrm{ClO}] = 2[\mathrm{ClO_2}]$ in the presence of excess [Cl]. The SF radicals were prepared using reaction (4), which has a rate constant[6] of $(1.8 \pm 0.2) \times 10^{-11}$ cm^3 s^{-1}. The F atoms are completely converted to SF radicals with excess [COS],

$$\mathrm{F + COS \rightarrow CO + SF.} \tag{4}$$

Unfortunately, the SF disproportionation reaction[6] has a rate constant of 2.6×10^{-11} cm^3 s^{-1},

$$\mathrm{2SF \rightarrow SF_2 + S,} \tag{5}$$

and some SF radicals are converted to SF_2 in the prereactor. Experiments were done for different $[\mathrm{SF}]/[\mathrm{SF_2}]$ ratios to show that the observed HF emission was from reaction (2) and that the H + SF_2 reaction was unimportant.

The major focus was on the ClO($X\,^2\Pi$), which has the $\{\ldots 5\sigma^2, 6\sigma^{*2}, 7\sigma^2, 2\pi^4, 3\pi^{*3}\}$ configuration with the unpaired π^* electron density polarized towards the O atom.[7] In principle, the reaction could proceed on the triplet surface with H adding directly to the O atom giving OH + Cl or by migration to the Cl end to form HCl + O(^3P). Direct attack on Cl via the triple surface is thought to have an activation barrier. Alternatively, the reaction may take place by addition on the singlet surface giving a bound HOCl intermediate. Dissociation to OH + Cl or to HCl + O(^3P) via a singlet–triplet curve crossing in the exit channel of the HClO configuration is possible. Dissociation to O(^1D) + HCl is 7.7 kcal mol^{-1} endoergic, see reaction (1c). The energy disposal pattern for the two product channels is needed to provide insight into dynamics of the H + ClO reaction. Several other chemical reaction systems involve the potential surfaces of HOCl (and/or HClO). These include the pioneering studies of Polanyi and Sloan on the Cl + OH(v) reaction,[8] the O(^1D) + HCl reaction,[9,11] the photochemistry of HOCl,[12] and the O(^3P) + HCl reaction, most recently studied for specific HCl rotational levels by Zare and coworkers.[13] Fortunately, some aspects of these surfaces are known from *ab initio* calculations.[14,15] Although formally similar, the H + SF reaction is rather different because of the thermochemistry and only the HF formation channel can be observed, since SH formation is nearly thermoneutral. The unpaired electron density in SF is more highly localized on S than on O for ClO, and the favored entrance channel presumably is the singlet HSCl configuration.

The importance of ClO chemistry to the upper atmosphere[16] makes understanding the H + ClO reaction of

 0021-9606/89/116223-11$02.10

practical significance, as well as an interesting example of competing multiple reaction pathways.

II. EXPERIMENTAL METHODS

The apparatus used in this work consisted of a main flow reactor for H atoms and a prereactor for generation of ClO and SF, see Fig. 1. The main flow reactor was of the same design as that described in our previous publications.[1,17] The flow time from the prereactor inlet to the IRCL observation zone was ~0.2 ms. The H atoms, prepared by a microwave discharge in a H_2/Ar mixture passing through the 8 mm Pyrex discharge tube (treated with *o*-phosphoric acid), were added at the front of the main flow reactor. Most of the Ar buffer gas was added through a perforated ring placed around the H atom inlet. The prereactor was a 15 mm diameter, 30 cm long Pyrex tube, that was attached to the main reactor via a four-jet inlet. The cross-sectional areas of the inlet tubes were selected by trial and error to obtain the flow speed of 25 m s^{-1} in the prereactor. The prereactor was provided with three equally spaced reagent inlets so that the residence time of the reactants ($Cl + ClO_2$ or $F + COS$) in the prereactor could be chosen as 10, 15, and 20 ms. The entrance of the prereactor was fitted with a Pyrex discharge tube for generating Cl and F atoms from flows of dilute Cl_2/Ar and of CF_4/Ar mixtures. The reagents were prepared and stored as 5% mixtures in Ar. Flow rates were measured with a combination of calibrated triflat flow meters, viscosity flow meters, and the pressure rise in bulbs of calibrated volume.

The IRCL was observed using a FTIR spectrometer (Digilab FTS-20) equipped with a liquid N_2 cooled InSb detector. Figure 2 shows a typical spectrum (1 cm^{-1} resolution) from the $H + ClO$ reaction. The individual vibrotational transitions of HCl and OH are resolved and their intensities were combined with the response function and the Einstein coefficients to obtain the relative populations. The OH Einstein coefficients were taken from Ref. 18, and those for HCl were calculated using an improved dipole moment function.[19]

Chlorine atoms were mixed with a flow of ClO_2 in the prereactor to generate ClO. If the ClO_2 was added at inlet C, the residence time in the prereactor was 20 ms. The [Cl] was estimated from the fractional dissociation of Cl_2 as follows. The $[H + H_2]$ in the main reactor was kept constant and the HCl emission intensity from the $H + Cl_2$ reaction was monitored with and without the MW discharge on the Cl_2 discharge line leading to the prereactor (see Fig. 1). The reduction in the HCl emission intensity gives an estimate of the fractional dissociation of Cl_2. Observations from several different days gave consistent results and for $[Cl_2] \leqslant 2\times10^{13}$ molecule cm^{-3}, the dissociation was 60 ± 10%. Thus, the [Cl] was taken as 1.2× the initial $[Cl_2]$. Reaction (3) is stoichiometric and $[ClO] = 2[ClO_2]$ for $[Cl] > [ClO_2]$. In order to know the [ClO] in the main reactor, it was necessary to control the [Cl] and $[ClO_2]$ in the prereactor. For the typical conditions used in these experiments, reagent flow of 1.0 μmol s^{-1} corresponded to 4.4×10^{12} molecule cm^{-3} in the main reactor and to 1.4×10 molecule cm^{-3} in the prereactor, due to the slower flow velocity in the later.

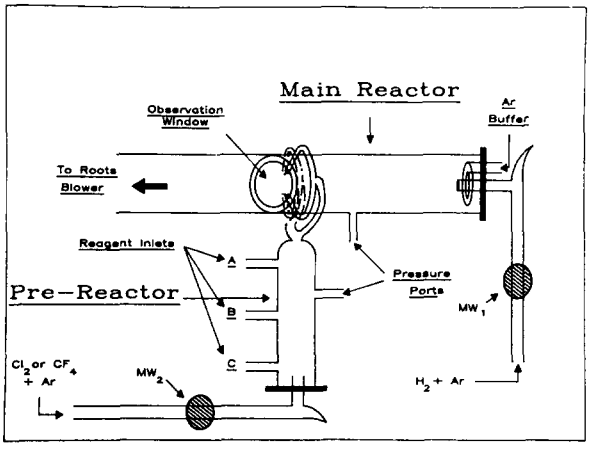

FIG. 1. Schematic diagram (not to scale) of the flow reactor with prereactor for generating ClO and SF.

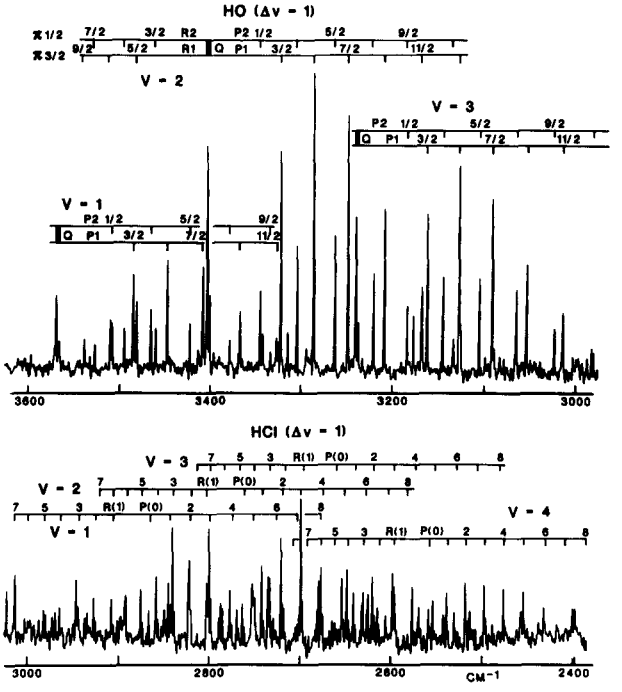

FIG. 2. The OH and HCl emission spectra from the H + ClO reaction. The $[H_2]$ was 8.3×10^{12}, [ClO] was 7.8×10^{12} molecule cm^{-3} and the Ar pressure was 0.7 Torr.

The SF radicals were produced by adding excess COS to F atoms, which were generated by passing CF_4 through the microwave discharge. From earlier measurements the [F] was taken as $2[CF_4]$.[20] The CF_4 source for F atoms was replaced by a discharge in SF_6 for a few experiments. Since F atoms react with H_2 to generate $HF(v \leqslant 3)$, excess COS was added to remove all the F atoms in the prereactor before the SF flow entered the main reactor. The residence time in the prereactor was varied by adding the COS at different inlets of the prereactor in order to change the $[SF]/[SF_2]$ ratio, i.e., to change the SF_2 formed by the SF disproportionation reaction. Observations from these variable $[SF]/[SF_2]$ ratio experiments are discussed in Sec. III.

III. RESULTS

A. The ClO reaction

1. The OH(v) distribution

Experiments first were done using an excess of [Cl] to ensure consumption of ClO_2 in the prereactor to obtain the OH vibrational distribution. However, $[Cl_2]$ was kept as low as possible in order to minimize or eliminate the HCl emission from the reaction of H atoms with the undissociated $[Cl_2]$. Experiments then were done using stoichiometric amounts of ClO_2 and Cl atoms. For $[ClO_2] = [Cl] = 1.0\times10^{14}$ molecule cm^{-3}, reaction (3) goes to $\geqslant 99\%$ completion after 20 ms of reaction time, since the rate constant is 5.9×10 cm^3 s^{-1}.

A typical emission spectrum with $OH(v\leqslant3)$ is shown in Fig. 2. The rotational and spin–orbit state distributions are 300 K Boltzmann. No emission from high J levels of $OH(v=1$ and $2)$ could be observed, however, this spectral region is *badly* overlapped by HCl emission and weak emission from high J levels might have been missed. Contribution to $OH(v)$ from the residual ClO_2 can be monitored from the $OH(v=4)$ emission, because ClO gives only $OH(v\leqslant3)$. For excess [Cl] in the prereactor, ClO_2 was completely converted to ClO because $OH(v=4)$ was never observed.

The first four experiments of Table I were done with four- to tenfold excess of [Cl] with $[H_2]\approx1.0\times10^{13}$ molecule cm^{-3}. The [ClO] in the main reactor was in the range of 1.8 to 8.0×10^{12} molecule cm^{-3}; the $OH(v)$ distribution did not show any dependence on [ClO] and P_1–P_3 was 30:41:29. Since the large [Cl] in experiments 1–4 could have caused some relaxation, experiments 5–8 were done with more nearly stoichiometric [Cl]; the [ClO] was in the range of 1.1 to 3.9×10^{12} molecule cm^{-3} in the main reactor or 3.4 to 12.1×10^{13} in the prereactor. For 5 and 6 the $[Cl]_0$ and $[ClO_2]_0$ were $\sim1.0\times10$ molecule cm^{-3}, and reaction (3) should have been $\geqslant97\%$ complete with a $[ClO_2]/[ClO]$ ratio of ≈0.01, as confirmed by the absence of $OH(v=4)$. Figure 3 shows a plot of P_V vs [ClO] for experiments 5–8; the average $OH(v)$ distribution was P_1–P_3 = 23:46:31.

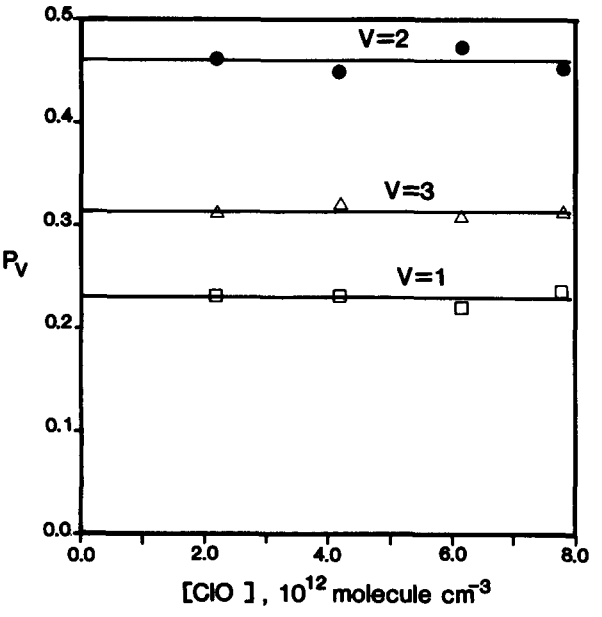

FIG. 3. Plot of $P_V(OH)$ vs [ClO] for the H + ClO reaction. The $P_V(OH)$ was independent of [ClO] in the range investigated; these-data are entries 5–8 in Table I.

Experiments 9–12 were done with excess ClO_2 in order to determine the $HCl(v)$ distribution, which will be given in

TABLE I. $OH(v)$ distribution from the ClO reaction.

Expt	$[H_2]$[a]	$[Cl_2]$[b] 10^{13} molecule cm^{-3}	$[ClO_2]$[b]	$P_v(OH)$ P_1	P_2	P_3	$\Sigma_v[OH(v)]$ arbitrary units
1	0.96	31.3	2.9	30.7	42.2	27.9	7.6
2			4.7	31.8	39.1	29.8	10.3
3			8.0	28.5	40.7	31.1	13.8
4			12.3	30.7	42.2	27.9	18.1
5	0.83	9.3	12.1	23.5	45.2	31.3	27.3
6		7.8	9.6	22.0	47.3	30.7	22.1
7	1.35	7.1	6.5	23.0	45.0	32.1	25.1
8		5.9	3.4	23.0	45.9	31.1	16.3
9[c]	1.04	9.6	10.9	26.4	44.4	29.2	13.0
10[c]		8.4	13.5	26.1	46.5	27.4	17.1
11[c]		8.4	14.6	24.5	46.7	28.8	15.7
12[c]		9.0	18.1	25.8	45.7	28.5	18.5
13	1.05	13.3	10.4	26.3	43.3	30.5	40.1
14		12.4	8.4	26.3	43.2	30.5	32.6
15		13.3	6.3	24.9	45.9	29.2	24.3
16		12.1	4.2	25.9	44.7	29.4	15.4
17		12.1	2.3	27.8	42.3	29.9	9.7

[a] The $[H_2]$ refer to main reactor; 88% dissociation is expected.

[b] Initial concentrations in the prereactor; $[Cl] = 1.2\times[Cl_2]$. The concentration in the reactor is 30 times lower.

[c] Experiments 9–12 were done with an excess of ClO_2 to obtain the HCl distribution. Since $OH(v=4)$ was observed in these experiments, the known $OH(v)$ distribution from the ClO_2 reaction and the $OH(v=4)$ intensity were used to calculate the contribution from the ClO_2 reaction, which was subtracted from the observed $P_v(OH)$ to obtain the distribution from ClO.

the next section, but the OH(v) distribution derived from these experiments are included here. Since the OH(v) distribution from the ClO_2 reaction is known,[1] P_1–P_4 = 19:28:28:25, the contribution to the OH(v = 1–3) concentration was computed using this distribution and the observed OH($v = 4$)]. The H + ClO_2 contribution was then subtracted from the observed [OH(v)] and the resulting distributions for H + ClO are shown in Table I. The average of these experiments gave P_1–P_3 = 26:46:28 in good agreement with experiments 5–8.

Experiments 13–17 were done to determine the OH formation rate constant from the ClO reaction relative to the ClO_2 and Cl_2 reactions; however, the OH(v) distributions are included in Table I. The $[Cl]_0$ was about equal to the $[ClO_2]$ for expt. 13, the $[ClO_2]$ was then progressively lowered in the series and $[Cl] \gg [ClO_2]$ for expt. 17. For each run the ClO_2 was completely converted to ClO, and the [ClO] was $2\times[ClO_2]$. The OH(v) distribution from this set of experiments was P_1–P_3 = 26:44:30.

The OH(v) distribution obtained from experiments 5–17 in Table I are quite reproducible, and the average corresponds to P_1–$P_3 = 26 \pm 3{:}44 \pm 2{:}30 \pm 2$. The surprisal plot was linear with $\lambda_v = -3.5$ (see Fig. 4) and P_0 was assigned from this plot. The nascent distribution is P_0–P_3 15.:22:38:25 with $\langle f_v \rangle = 0.45$. In experiments based upon observing H + ClO as a secondary reaction,[1] the OH(v) distribution was estimated as P_1–$P_3 = 40 \pm 8{:}40 \pm 8{:}20 \pm 4$, which is in modest agreement with the more reliable results presented here.

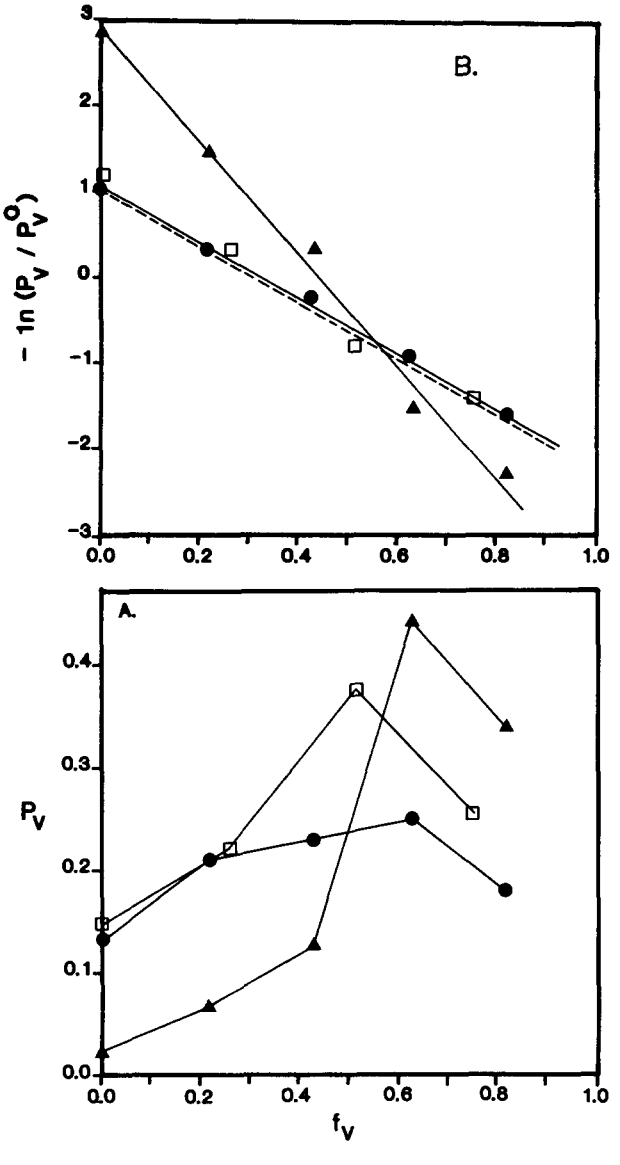

FIG. 4. (a) Plots of P_v(OH) vs f_v for the H + ClO (●) and O(^1D) + HCl (▲), Ref. 9, reactions. The OH(v) distribution from the trajectory calculations (□), for O(^1D) + HCl, Ref. 15, also is shown. (b) Surprisal plots for the OH(v) distributions from the H + ClO and O(^1D) + HCl reactions; the larger $\langle E \rangle$ for O(^1D) + HCl should be remembered in comparing the results.

2. The HCl(v) distribution

Emission from HCl(v = 1-4) is clearly evident in Fig. 2. Trace levels of emission from $v = 5$ might have been present in some experiments, but assignment was not certain. The HCl($v = 5$) level corresponds to 38.3 kcal mol^{-1}, which requires all of the available energy $\langle E \rangle$. The HCl(v) rotational distributions were 300 K Boltzmann. The HCl(v) distribution was measured using either an excess of ClO_2 or nearly stoichiometric amounts of Cl and ClO_2. Table II lists experiments for three different $[H_2]$. For experiments 1–4 the $[Cl_2]$ and $[ClO_2]$ were nearly equal and the estimated [ClO] in the main reactor varied from 2.0 to 8.0×10^{12} molecule cm^{-3}. Since the background spectra (i.e., the IRCL without the added ClO_2) did not show any HCl emission, the observed HCl emission was assigned only to the H + ClO reaction. The vibrational distribution was independent of [ClO] with P_1–P_4 = 30:36:21:13. Experiments 5–8 were done with excess of ClO_2 and $[H_2] = 1.0\times10^{13}$ molecule cm^{-3}, the $[ClO_2]$ in the reactor varied from 3.2 to 6.0×10^{12} molecule cm^{-3}. The HCl(v) distribution was invariant with $[ClO_2]$, and P_1–P_4 = 36:34:16:13. For this series the Σ_vHCl(v) did not vary with $[ClO_2]$ indicating that [Cl] was the limiting reagent in each experiment. The average of the eight experiments is P_1–$P_4 = 33 \pm 3{:}35 \pm 2{:}19 \pm 3{:}13 \pm 1$. Experiments, based upon observing H + ClO as a secondary reaction,[1] gave P_1–P_4 = 37:33:19:11 in agreement with the distribution reported here. The surprisal plot for this vibrational distribution is not linear (see Fig. 5), and P_0 was estimated from the P_v vs f_v plot. Although P_0 is rather uncertain, the selected distribution is P_0–P_4 = 24:25:27:16:8 with $\langle f_v \rangle = 0.31$.

3. OH/HCl branching ratio

The data summarized in Table III were used to calculate the branching ratio [the OH(v) distributions and the Σ[OH(v)] from these experiments are entries 5–12 in Table I and similar results for the HCl(v) channel are given in entries 1–8 of Table II]. For experiment 1–4 the ClO_2 was completely removed, as judged by the absence of any OH($v = 4$) emission. Therefore, the observed OH and HCl arise only from ClO and the branching ratio is obtained directly. For the experiments with ClO_2 in excess, experiments 5–8, the [OH] from the ClO_2 reaction was subtracted from

TABLE II. HCl(v) distribution for the ClO reaction.

Expt.	$[H_2]^a$	$[Cl_2]^b$	$[ClO_2]^b$	P_v (HCl)			Σ_v [HCl(v)] arbitrary units
	10^{13} molecule cm^{-3}		P_1	P_2	P_3	P_4	
1	0.83	9.3	12.1	28.0	36.0	23.0	13.0	5.3
2		7.8	9.6	31.0	35.0	20.0	14.0	4.4
3	1.35	7.1	6.5	30.0	38.0	21.0	11.0	4.9
4		5.9	3.4	32.0	35.0	20.0	13.0	3.8
5	1.04	9.6	10.9	36.0	34.0	17.0	13.0	2.8
6		8.4	13.5	36.0	35.0	15.0	13.0	3.1
7		8.4	14.6	37.0	34.0	16.0	13.0	3.3
8		9.0	18.1	36.0	33.0	17.0	14.0	3.5

[a] The H_2 concentration in the reactor. The [H] can be estimated from the expected 88% dissociation.
[b] The Cl_2 and ClO_2 concentration in the prereactor. These values are reduced by a factor of 30 in the reactor.

the total [OH] in order to determine the OH/HCl branching. The procedure was as follows. The OH($v \leqslant 3$) contribution from the ClO_2 reaction, calculated from the OH($v = 4$) population, was subtracted from the $[OH(v \geqslant 1)]_{total}$ to obtain $[OH]_{ClO}$. Based on the observed OH($v = 4$)], the estimated $[OH]_{ClO}/[OH]_{ClO_2}$ ratios were 5.8, 3.5, and 3.2 for expts. 6, 7, and 8, respectively. This was counterchecked by calculating the expected [OH] using the $[ClO]/[ClO_2]$ in the reactor and their respective rate constants for OH formation. Based on 60% dissociation of Cl_2, the $[ClO_2]$ should have been in excess of [Cl] by 3.5, 7.3, and 4.5×10^{13} molecule cm^{-3}, which corresponds to $[ClO]/[ClO_2] = 5.7, 3.0,$ and 4.4 for experiments 6, 7, and 8, respectively. For $k_{ClO}/k_{ClO} = 1.0/1.3$, *vide infra*, the $[OH_{ClO}]/OH_{ClO}]$ ratios would be 4.6, 2.4, and 3.5, respectively, which is in a fair agreement with the ratios obtained from the $[OH(v \geqslant 1)]_{total}$ and the [OH($v = 4$)]. Although $[ClO_2]_0$ and $[Cl]_0$ should have been approximately equal for experiment 5, OH($v = 4$) was observed, suggesting that ClO_2 was not completely converted to ClO. The low [HCl] from this experiment, even though the $[ClO_2]$ was highest, indicates that the effective [ClO] was less than that expected, and the Cl_2 dissociation must have been $< 60\%$. Finally the $[OH(v \geqslant 1)]/[HCl(v \geqslant 1)]$ ratios were scaled to account for the P_0 contributions, and the overall product ratios were obtained as given in the last column of Table III. The average of the eight experiments gave an OH/HCl branching ratio of 4.5 ± 0.3.

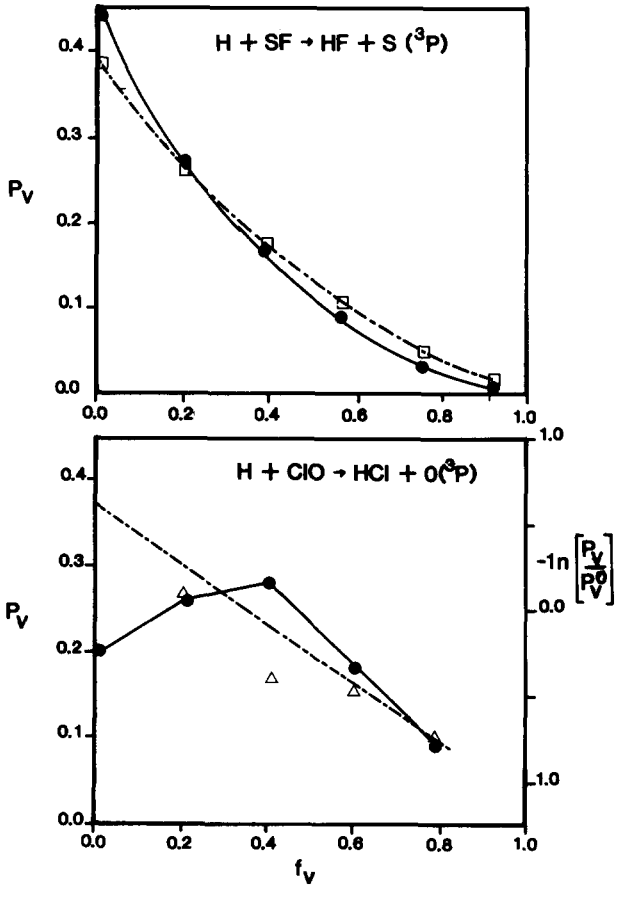

FIG. 5. Comparison of the HCl(v) and HF(v) distributions from H + ClO and H + SF. The surprisal plot (△ and ---) is included for the HCl(v) distribution to demonstrate the nonlinearity. Within the experimental uncertainty, the HF(v) distribution from H + SF matches the prior distribution (□ and ---).

4. The ClO rate constant

The OH($v \geqslant 1$) formation rate constant was measured relative to the rate constants for both H + Cl_2 (2.06×10^{-11} cm^3 s^{-1}) and H + ClO_2 (7.8×10^{-11} cm^3 s^{-1}).[1] When the discharge on the Cl_2 flow to the prereactor is off, the Cl_2/Ar flow becomes a second reagent flow. Therefore, the H + Cl_2 and ClO_2 reactions could be observed simultaneously. The ClO reaction then was observed when the discharge on the Cl_2/Ar line was turned on. The plots of [OH] vs [ClO] and $[ClO_2]$ and [HCl] vs $[Cl_2]$ are presented in Fig. 6. The experiments were done for a constant $[H_2]$ of 1.0×10^{13} molecule cm^{-3}; see expts. 13–17 in Table I. Comparison of the Σ[OH(v)] from ClO_2 to that from ClO gives a rate constant ratio of 1.3 ± 0.3. The rate constant ratio with respect to the Cl_2 reaction was 2.6 ± 0.5. Thus, the OH($v \geqslant 0$) formation rate constants (based on $P_0 = 0.15$) from the measurements with Cl_2 and ClO_2 were $(6.2 \pm 0.6) \times 10^{-11}$, and $(6.3 \pm 0.6) \times 10^{-11}$ cm^3 s^{-1}, respectively. From the branching ratio of 4.5, the HCl formation rate constant is 1.4×10^{-11} cm^3 s^{-1} and the total rate constant becomes $(7.7 \pm 1.9) \times 10^{-11}$ cm^3 s^{-1}.

TABLE III. OH/HCl branching ratio for the ClO reaction.

Expt.	[HCl]	$[OH(v\geqslant 1)]_{total}$	$[OH(v\geqslant 1)]_{ClO_x}$	$[OH]_{ClO}$	[OH]/[HCl] ($v\geqslant 1$)	[OH]/[HCl] ($v\geqslant 0$)
1	5.33	27.26	···	27.26	5.11	4.6
2	4.39	22.11	···	22.11	5.04	4.6
3	4.91	25.07	···	25.07	5.10	4.6
4	3.79	16.28	···	16.28	4.30	3.9
5	2.77	16.35	3.32	13.03	4.70	4.3
6	3.11	20.09	2.98	17.11	5.50	5.0
7	3.30	20.59	4.90	15.69	4.74	4.3
8	3.51	23.83	5.33	18.50	5.27	4.8
						Average = 4.5 ± 0.3

B. The SF reaction

Before the results are presented, other reactions that could interfere with observation of the H + SF reaction must be considered. The main reactor contains H atoms and undissociated H_2 with $[H]/[H_2]\approx 15$.[1] The microwave discharge through CF_4 produces mainly CF_2 radicals and F atoms, along with a small amount of CF_3 radicals. Reactions that must be evaluated for contribution to HF formation are

$$F + H_2 \rightarrow HF + H; \quad \Delta H_0^\circ = -34.0 \text{ kcal mol}^{-1}. \tag{6}$$

$$F + H + M \rightarrow HF + M; \quad \Delta H_0^\circ = -135.4 \text{ kcal mol}^{-1}, \tag{7}$$

$$H + CF_3 \rightarrow HF + CF_2; \quad \Delta H_0^\circ = -48.7 \text{ kcal mol}^{-1} \tag{8}$$

$$H + CF_2 \rightarrow HF + CF; \quad \Delta H_0^\circ = -13.0 \text{ kcal mol}^{-1}. \tag{9}$$

Reactions (6) and (7) can be ignored, if all the F atoms are converted to SF by excess COS. The rate constants for reactions (8) and (9) are $(8.9 \pm 1.8)\times 10^{-11}$ and $(1.6 \pm 0.4)\times 10^{-13}$ cm^3 s^{-1}, and the available energies can give HF(v) up to $v = 4$ and $v = 1$, respectively. Although, reaction (8) has a large rate constant, the CF_3 concentration from the CF_4 discharge is low. Furthermore, the reaction gives a declining HF(v) distribution, P_1–P_3 = 84:10:06[22,23] and the contributions from reactions (8) and (9) should mainly be HF($v = 1$). A series of empirical tests were done to check for possible interference from these reactions using $[CF_4]$ and $[H_2]$ of 7.8×10^{12} and 1.2×10^{13} molecule cm^{-3}, respectively: (1a) Microwave discharge on the CF_4 line to the prereactor active, but the microwave discharge on the H_2 line off. (1b) Same conditions as in (1a), but with excess COS added to the prereactor. (2a) Both discharges on the CF_4 and H_2 lines active, but no COS added to the prereactor. (2b) The discharges on both CF_4 and H_2 lines active, but a large excess of COS added to prereactor. The HF(v) distribution from (1a) was P_1–P_3 = 15:54:31 in accord with the known distribution from reaction (6).[24] When COS was added in sixfold excess to the prereactor, no HF emission was observed because the F atoms were removed. With the discharge on both lines active, but in the absence of COS, the entire 4200 to 2400 cm^{-1} region was filled with HF($v < 10$) emission. This emission is not compatible with reaction (8) and reaction (7) must be responsible. When excess COS was added to the prereactor to remove F atoms, emission from the higher HF(v) levels vanished and the spectrum of Fig. 7 was obtained. Experiments were also done using SF_6 as the F atom source for condition (2a) and a similar HF(v) distribution was observed, indicating that the H + CF_3 and CF_2 reactions are not major contributors to HF(v) formation. For condition (2a) most of the HF($v\geqslant 3$) emission must arise from the three-body reaction between F and H atoms.[23]

If excess COS is added to remove F atoms, there should not be any extraneous contribution from HF(v) emission, and the HF emission can be assigned to the H + SF reaction (after the possibility of H + SF_2 has been eliminated). This claim has been further documented by independently[23] studying the H + CF_3 reaction in the present flow reactor; the HF(v,J) distributions do not resemble any of the distributions observed during the H + SF study.

The next question to resolve is the role, if any, of SF_2. A typical spectrum from H + SF is shown in Fig. 7; emission from HF($v\leqslant 5$) is observed with declining intensity for increasing v. The unusual aspect of this spectrum is the high

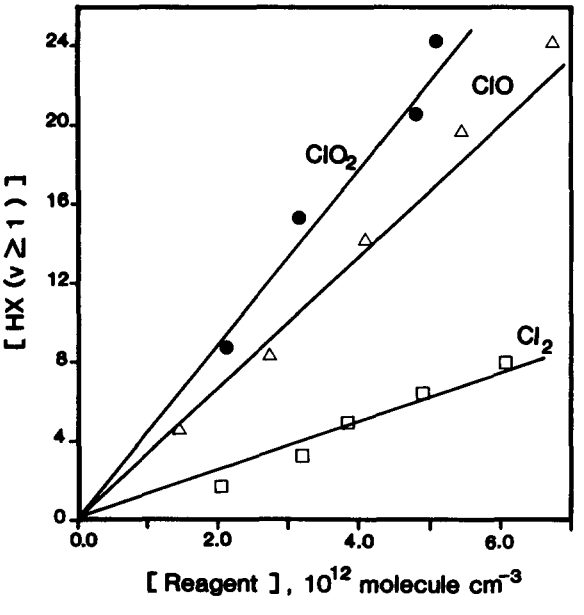

FIG. 6. Plots of [HX($v\geqslant 1$)] (X = Cl,O) vs [reagent] for the ClO, $ClO_{2,3}$ and Cl_2 reactions. The $[H_2]$ was 1.0×10^{13} molecule cm^{-3} for all three cases.

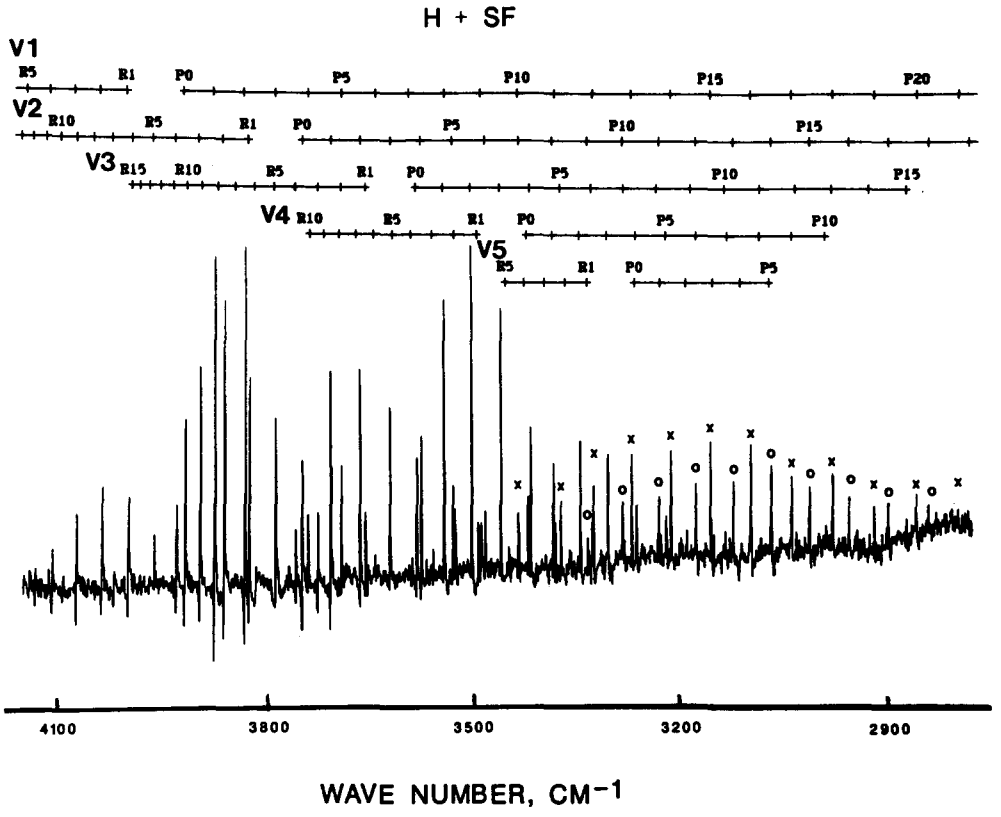

FIG. 7. The HF($\Delta v = 1$) spectrum from the H + SF reaction. The initial [CF_4] and [COS} in the prereactor were 5×10^{13} and 1.9×10^{14} molecule cm^{-3}; the [H_2] in the reactor was 6.2×10^{12} molecule cm^{-3}. The x and o symbols identify the high J lines of $v = 1$ and 2, respectively.

fraction of rotationally excited HF($v = 1,2$) molecules. A summary of the experiments for the H + SF reaction system is given in Table IV. Experiments were done for three different [H_2] and the [CF_4] was varied from 1.5 to 9.0×10^{13} molecule cm^{-3}. The COS was in fivefold excess of [CF_4] for most of the experiments, which gives $\geqslant$95% consumption of the [F] for a reaction time of 20 ms. The absence of F atoms was confirmed as follows. First, the F + H_2 reaction

TABLE IV. HF(v) distribution for the SF reaction.

Expt.	$\frac{[H_2]^a}{10^{12}}$	$\frac{[CF_4]^b}{10^{13}}$ molecule cm^{-3}	$\frac{[COS]^b}{10^{14}}$	Vibrational distribution[c] P_1	P_2	P_3	P_4	P_5	ΣHF(v)
1	8.4	8.9	4.7	50.4 0.47	30.5 0.26	14.7 0.07	4.4	1.0	9.6
2	8.4	8.9	2.2	50.0 0.51	31.4 0.27	14.2 0.05	4.4	1.0	6.7
3	8.4	3.8	2.1	47.5 0.44	31.4 0.26	15.0 0.05	6.1	trace	4.6
4	6.2	5.0	1.9	48.6 0.50	31.9 0.26	14.9 0.04	4.6	trace	6.3
5	6.1	1.5	1.1	50.6 0.50	31.2 0.29	13.5 0.00	4.7	trace	3.9
6[d]	26.0	1.4	0.8	55.0 51.2	29.4 31.7	12.01 12.1	3.5 5.0	trace trace	2.7
7[d]	26.0	2.3	1.1	49.7 55.1	32.3 29.9	12.9 11.3	5.0 3.2	trace trace	4.1

[a] The [H_2] is for the main reactor.
[b] These concentrations refer to the initial concentrations in the prereactor. See the text for the ratio of SF to SF_2 entering the reactor for a prereactor residence time of 20 ms.
[c] The second entry is the fraction of the population in the high J levels for expts. 1 to 5. For 6 and 7 the second entry is the vibrational distribution for 10 ms residence time in the prereactor.
[d] The first and second entries are for adding COS at inlets A and C of the prereactor, corresponding to reaction times of 20 and 10 ms, respectively; see the text.

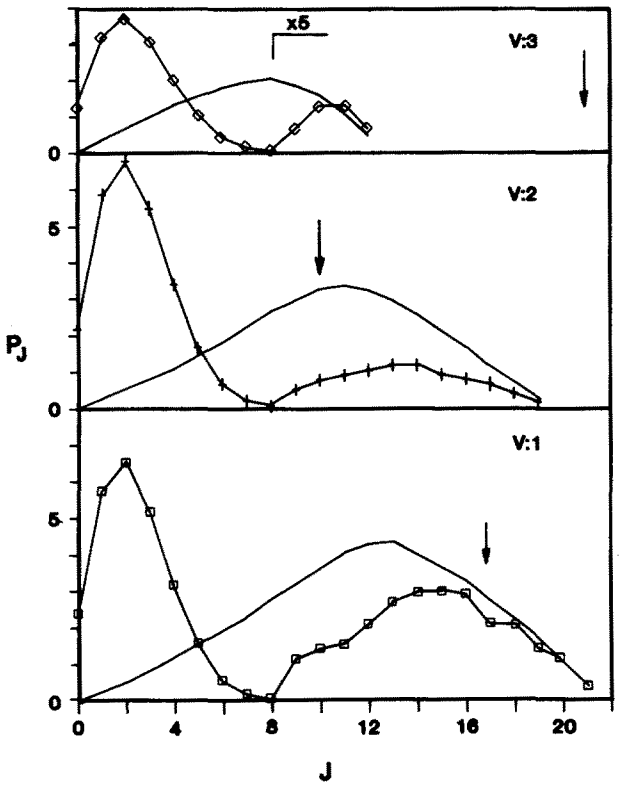

FIG. 8. Plots of P_J(HF) vs J for the H + SF reaction. The solid lines without points are our estimates of the nascent HF(v,J) distributions. The $\Sigma_J P_{vJ}$ values are normalized to the average P_v values. Note the scale expansion for $J>8$ for $v=3$. The arrows denote the thermochemical limits for S(^1D) formation for $v=1$ and 2 and for S(^3P) formation for $v=3$.

was observed by mixing F atoms from the prereactor with the H_2 in the main reactor while the discharge on the H_2 line was off. Next excess [COS] was added to the prereactor, the HF emission from F + H_2 was removed, indicating that the F atoms had been consumed by reaction (4). Unfortunately, reaction (5) has a rate constant of 2.6×10^{-11} cm^3 s^{-1} and a significant amount of the SF is converted to SF_2 during the 20 ms residence time in the prereactor. For experiments 1–5 the [SF_2]/SF] ratio, as calculated by numerical integration of the rate equations, varied from 7 to 42, but the observed HF(v,J) distribution was the same for each experiment. In order to further reduce the [SF_2]/SF] ratio, COS was added at inlet A or C, corresponding to 10 and 20 ms residence time in the prereactor for experiments 6 and 7. The calculated [SF_2]/SF] ratios were 4.5 and 9.8 for experiment 6, and 2.6 and 5.7 for experiment 7 for the 10 and 20 ms residence times, respectively. Although the SF_2/SF ratio was varied by a factor of 5, the observed HF(v) distribution was the same for the experiments listed in Table IV. The ΣHF(v)] showed, a strong dependence on the [CF_4] for excess [COS], although not strictly first order, indicating the expected dependence on [SF]. The HF(v = 1) from the background spectra, i.e. the HF($v=1$) from H + CF_3 and CF_2 were always less than 10% of that from the SF reaction. Therefore, interference from H + CF_3 or CF_2 reactions can not affect the HF(v) distribution reported here. The average HF(v) distribution from all the experiments was P_1-P_5 = 49.4 ± 1.0:31.6 ± 0.5:14.6 ± 0.6:4.8 ± 0.6:trace. As shown in Fig. 5, the HF(v) distribution is indistinguishable from the prior (statistical) distribution. Therefore, P_0 was obtained from comparison with the statistical distribution and the renormalized distribution is P_0–P_5 = 44:28:18:9:1 with $\langle f_V \rangle = 0.20$.

Although [SF_2] was larger than [SF] for all experiments in Table IV, we claim that the observed HF(v,J) emission was from the H + SF reaction and *not* from H + SF_2. Additional arguments can be made to support this claim besides the invariance of the HF(v,J) distribution with [SF_2/SF_4]. One is the small rate constant expected for H + SF_2, which can be estimated, using the 10^{-3} smaller rate constant for OF_2 vs OCl_2 and the known rate constant for SCl_2 (1.5×10^{-11} cm^3 s^{-1})[1,26a] for reference. The rate constant for H + SF_4 also is small.[26b] Secondly, the HF(v,J) distribution for H + SF_2 would be expected to resemble those for direct H atom reactions and be sharply peaked around $f_V \approx 0.30$.[4] The distribution assigned to the H + SF certainly does not have this form.

Very high HF(v) rotational excitation was observed, as shown in Fig. 8, and the fractions in the high J envelopes are 0.5, 0.3, and 0.05 for $v=1$, 2, and 3, respectively. The high-

TABLE V. Summary of the energy disposal for the H + ClO and SF, and O(^1D) + HCl reactions.

Reaction	$\langle E \rangle$[a]	Vibrational distribution P_0	P_1	P_2	P_3	P_4	P_6	λ_V	$\langle f_V \rangle$	Comments
H + ClO	38.7	15	22	38	25	···		− 3.5	0.45	OH channel[b]
	39.7	24	25	27	16	8		c	0.31	HCl channel[b]
O(^1D) + HCl	46.4	2	7	13	44	34	···	− 6.4	0.63	OH channel[b,d]
	47.4	2	4	15	17	40	23	− 6.0	0.59	HCl channel[d]
	46.4	13	21	23	25	18	···	− 3.2	0.45	OH channel[e]
H + SF	56.3	44	27	17	8	3	1	0.9	0.20	HF channel[f]

[a] Available energy in kcal mol^{-1}.
[b] The rotational energy distributions are not available for the H + ClO reaction. The OH rotational excitation OH($v=0$ and 1) is very high for O(^1D) + HCl (Ref. 11).
[c] The surprisal plot was not linear for the HCl channel, see the text.
[d] Taken from the low pressure IRCL experiments, Ref. 9.
[e] Trajectory calculation for a potential fitted to the *ab initio* ground state surface, Ref. 15.
[f] The $\langle f_R \rangle$ for H + SF is 0.22.

est observed J levels were 21, 19, and 12, which can be compared to the thermochemically limiting values of 27, 24, and 20, for $v = 1$, 2, and 3, respectively, suggesting a possible angular momentum constraint on the HF(v,J) rotational excitation. The nascent rotational distributions in Fig. 8 were estimated by truncating the Boltzmann distribution and redistributing the population into the mid J levels. A detailed procedure and discussion about validity of such estimates of the nascent rotational distributions is given in Ref. 27 and 17. Based on the estimated distributions in Fig. 8 and assignment of $\langle f_R \rangle = 0.27$ for HF($v = 0$), the overall $\langle f_R \rangle$ was calculated as 0.22. Neither the vibrational nor rotational distributions of HF show any indication of a two-component nature, and there is no evidence for a significant contribution from reaction (2a).

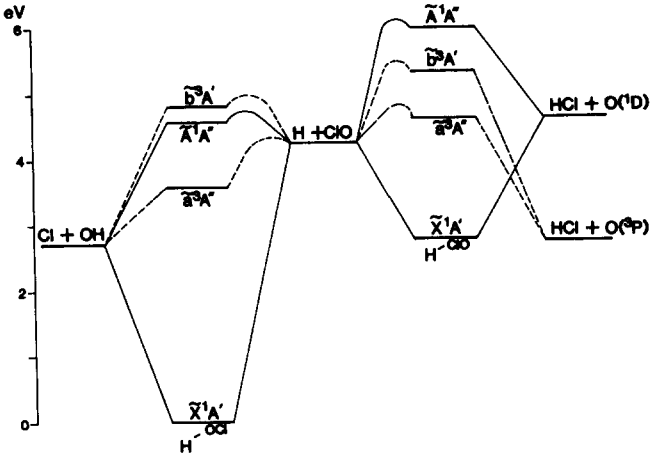

FIG. 9. Correlation diagram for the H + ClO system. The relative energies of HOCl($^1A'$) and HClO($^1A'$) are for their equilibrium geometries as given in Ref. 14. The relative energies shown for the other states are for the same geometry. The implied barriers for reaching the $\tilde{a}$ surface from H + ClO are for collinear geometry.

IV. DISCUSSION

A. The ClO reaction

The energy disposal for H + ClO, which favors the OH channel over the HCl channel by a factor of 4.5, is summarized in Table V. The OH vibrational distribution, P_0–P_3 = 15:22:38:25, gives a linear surprisal plot with $\lambda_V = -3.5 \pm 0.6$. The HCl(v) distribution, P_0–P_4 = 24:25:27:16:8 with $\langle f_V(\mathrm{HCl}) \rangle = 0.31$, does not fit a linear surprisal (see Fig. 5). The vibrational energy disposal to the OH and HCl channels is clearly different. If there is a small direct component to the HCl channel that mainly gives P_2 and P_3, then the remaining distribution might give a linear surprisal with a small $-\lambda_V$. However, this is conjecture. Formation of HCl($v = 5$) corresponds to $f_V = 0.96$, but P_5 was below the limit of reliable assignment. Since the observed rotational distributions for both HCl and OH were 300 K Boltzmann, no conclusions can be reached about rotational energy disposal, except that the OH($J \geqslant 10$) levels are not favored.[1] This broad restriction suggests that $\langle f_R(\mathrm{OH}) \rangle$ is less than 0.10–0.15. Since rotational relaxation of HCl is even more rapid than OH, not even a limit can be given for the rotational energy disposal to the HCl channel.

Figure 9 is a correlation diagram for H + ClO, which shows the two product channels and the lowest energy singlet and triplet states of HOCl and HClO. The energies selected for the excited states are for the equilibrium geometries of HOCl($\tilde{X}\,^1A'$) and HClO($X\,^1A'$) of Ref. 14. Four surfaces, $^1A'$, $^1A''$, $^3A'$, and $^3A''$, arise from H(^2S) + ClO($^2\Pi$). The lowest triplet state, $\tilde{a}\,^3A''$, and the ground state, $\tilde{X}\,^1A'$, for the HOCl configuration are below the H + ClO energy. In viewing the diagram it should be remembered that the much more rapid motion of the H atom, relative to the motions of the Cl and O atoms, provides an opportunity for the H atom to migrate between the Cl and O atoms before the heavy atoms separate on either the triplet or singlet surfaces. For collinear approach, the $1s_H$ orbital will overlap the σ^*_{ClO} orbital and the reaction could follow the $\tilde{a}^3A''$ repulsive surface corresponding to the HOCl or HClO configurations. According to the calculated results for the triplet potential, the H atom would attack only the O atom for room temperature conditions, because the end-on approach to Cl would have a barrier of $\sim$9 kcal mol^{-1}. Although the $\tilde{a}\,^3A''$ surface has a shallow minimum for the bent H–OCl structure,[14] it is basically a repulsive surface with respect to the Cl–O bond. For reaction on the $\tilde{a}\,^3A''$ surface, OH formation would be the direct channel and HCl formation would be the result of migration. The OH(v) distribution from reaction on the $\tilde{a}$ potential should resemble those for direct H atom reactions on repulsive potentials, i.e., the distribution would be sharply inverted and not extend to the thermochemical limit,[1,27,28] and the HCl(v,J) distributions should be similar cases of migratory dynamics.[28,29] These expectations are not in accord with our experimental OH(v) and HCl(v) distributions.

For noncollinear approach, the $\tilde{X}\,^1A'$ potential is favored for both the HOCl or HClO configurations. Formation of OH + Cl occurs by adiabatic dissociation on the HOCl($\tilde{X}\,^1A'$) surface. Formation of HCl($^1\Sigma^+$) + O(^3P) must involve a crossing from the HOCl($^1A'$) or HClO($^1A'$) surface to the ($\tilde{a}\,^3A''$) surface. The OH(v) vibrational distribution resembles that for the H + ClO_2 reaction,[1] and it is consistent with reaction via a short lived, bound intermediate. A trajectory calculation[15] on the fitted *ab initio* HOCl($\tilde{X}\,^1A'$) surface has been reported for O(^1D) reacting with HCl. The calculated OH(v) distribution, as well as the surprisal plot, are compared to our experimental results and to the O(^1D) + HCl experimental results in Fig. 4 (also see Table V). The general pattern of OH(v) distributions from the trajectory calculations and our H + ClO results are quite similar with $\lambda_V = -3.2$ and -3.5, respectively. We take this as strong evidence that formation of OH + Cl proceeds via the $\tilde{X}\,^1A'$ potential surface.

The O(^1D) + HCl reaction has been studied by several groups and all three product channels, viz. H + ClO, OH + Cl, and HCl + O(^3P) have been observed.[10] The branching between OH and HCl favors the OH channel by a factor of 7, according to the atomic (O and H) resonance fluorescence detection technique,[10] and by a factor of 20 from the low pressure IRCL experiments.[9] Formation of H + ClO contributes $\sim$20% to the overall reaction. The

OH(v,J) distributions determined by the LIF experiments[11] indicated that $P_1/P_0 = 1.5$; rotational excitation is high and the populations extend up to the thermochemical limit for $v = 0$ and 1. The IRCL results,[9] see Table V, show that the OH(v) and HCl(v) distributions are both sharply inverted with a maximum in $v = 3$ and 4, respectively. Both distributions give $\langle f_V \rangle$ values near 0.6 and the vibrational surprisal plots are linear with large $-\lambda_V$ values. The contrast in energy disposal between the H + ClO and O(^1D) + HCl reactions is marked, considering that both presumably involve states of HOCl as an intermediate. Sloan and co-workers[9] explained their distribution as a consequence of the reaction proceeding via the excited HOCl($^1A''$) potential entered by the O–HCl configuration. However, it is not obvious why entrance to the $\tilde{X}\,^1A'$ surface should be blocked.

The trajectory calculation for O(^1D) + HCl give $\langle f_R(\mathrm{OH}) \rangle = 0.30$, which is much higher than our estimate of the limit for $\langle f_R(\mathrm{OH})$ for H + OCl, but consistent with experimental results for O(^1D) + HCl.[11] An interesting, and presently unresolved, question is whether entrance to the $\tilde{X}\,^1A'$ surface via O(^1D) inserting into HCl gives different rotational energy disposal than for entrance via H + OCl. The mean orbital angular momenta for the two methods of HOCl formation at room temperature are $\sim 4\hbar$ and $35\hbar$, based upon the thermal rate constants (0.77×10^{-10} and 1.5×10^{-10} cm^3 s^{-1}) for H + OCl and O(^1D) + HCl,[10] respectively. If L is converted to $\mathbf{J}'_{\mathrm{OH}}$, the O($^1D$) reaction will favor high rotational states of OH. On the other hand, the average $\mathbf{J}_{\mathrm{ClO}}$ is $\sim 20\hbar$, whereas $\mathbf{J}_{\mathrm{HCl}}$ is only $\sim 5\hbar$ and $\mathbf{J}_{\mathrm{Total}}$ is not so different for the two reactions.

An extensive literature is associated with measuring and trying to understand the vibrational and rotational distributions of OH from O(^1D) reacting with H_2 and small hydrocarbons.[30,31] The rotational and vibrational distributions are more inverted than anticipated based upon an insertion mechanism. The recent data for O(^1D) + HCl follow this trend. The rotational excitation from O(^1D) + HCl has been explained as a consequence of excitation of the bending mode of HOCl during the insertion process. However, a Monte Carlo simulation of this reaction using a RRKM model with the angular momentum constraint applied at the point of separation of the products suggests that the OH rotational excitation just arises from the large orbital angular momentum in the entrance channel and has no unique dynamical origin.[31f] Similar discussions have been given for the O(^1D) + H_2 reaction.[31e] Trajectory calculations with various types of potentials have shown that the distributions from O(^1D) + H_2 are not very dependent on details of the potential surfaces. Experimental definition of the OH(v) rotational distributions from both H + ClO and (^1D) + HCl together with additional model calculations could help resolve the remaining question about rotational energy disposal.

Formation of HCl + O(^3P) from $\tilde{X}\,^1A'$ must involve a surface crossing to $\tilde{a}\,^3A''$ in the exit channel. The calculations[14] indicate that such a crossing exists for bent H–ClO at R(Cl–O) $\approx$ 3.45 a.u. The equilibrium ClO bond length is 3.0 a.u.for the radical[32] and $\approx$3.2 a.u. for the HOCl or HClO molecules.[14] The experimental HCl(v) distribution is characteristic of a process involving a short lived intermediate and the results are consistent with a surface crossing mechanism in the exit channel. The HCl channel from H + OCl is analogous to HF formation from the F + OH reaction, studied by Sloan and co-workers.[33] The HF(v) distribution declined with increasing v. In this case, HF + O(^3P) is the only thermochemically allowed exit channel, and the mechanism was assigned as proceeding through HO$F(\tilde{X}\,^1A')$ with a singlet–triplet crossing in the exit channel.

If the H + ClO reaction proceeds via the HOCl($\tilde{X}\,^1A'$) surface, questions arise about the interpretation of the role of vibrational energy in the Cl + OH(v) reaction.[8] According to microscopic reversibility, the Cl + OH(v) reactants must readily sample the HOCl($\tilde{X}\,^1A'$) potential and HCl would be formed by crossing to the H–ClO triplet potential in competition with dissociation back to OH + Cl. Possibly some reactant pairs pass over the repulsive HOCl($\tilde{a}\,^3A''$) surface, but we see no reason that this pathway should dominate over reaction via the singlet surface. Reliable information about the intersection seam for the $\tilde{a}$ and $\tilde{X}$ potentials is needed. The role of vibrational energy in the Cl + OH(v) reaction probably needs reinterpretation[8] in view of the multiple reaction pathways.

B. The SF reaction

The HF + S(^1D) and HF + S(^3P) channels are exoergic by 29.7 [HF($v\leqslant2$)] and 56.1 [HF($v\leqslant5$)] kcal mol^{-1}, respectively, whereas the corresponding HCl + O(^1D) channel was endoergic for the ClO reaction. Neither the rotational nor vibrational distributions show any indication of a bimodal nature, and the energy disposal pattern shows no evidence for S(^1D) formation. The HF(v) distribution is nearly statistical. The $\langle f_R(\mathrm{HF}) \rangle$ was estimated as $\sim$0.22; however, the $\langle g_R \rangle$ values for each level tend to be similar. The mean fraction released as translational energy is $\sim$0.6. The rotational distributions do not extend to the thermochemical limit and there probably is a dynamical constraint to formation of high angular momentum HF states. Although the $\langle f_R(\mathrm{HF}) \rangle$ is less than the statistical value, the rotational energy disposal from reaction (2a) probably is higher than for reactions (1a) and (1b). The correlation diagram for H + SF would be similar to that for H + ClO, except that the binding for the HSF electronic states is less and the exit channels have different thermochemistry. The $\tilde{X}\,^1A'$ surface can lead directly to SH + F or HF + S(^1D); formation of HF + S(^3P) requires a singlet–triplet surface crossing. Since the SH formation channel is nearly thermoneutral, branching to this channel would be small relative to HF + S(^1D) formation. The formation of S(^1D) has not been experimentally disproven, but there is no evidence in favor of it. The nonadiabatic crossing to the triplet surface from HSF($\tilde{X}\,^1A'$) appears to be facile and HF + S(^3P) formation is dominant.

The energy disposal pattern for H + SF seems to resemble an elimination reaction[25,34,35] much more than does the HCl channel from H + ClO. It is for this reason that we

identified HCl–O *dissociation* as the reaction mechanism for the latter with the singlet–triplet crossing occuring late in the exit channel. Two quite major differences in the H + SF thermochemistry, relative to H + OCl, are important. D(H–SF) is less than D(H–OCl) and the HF + S(^3P) channel is much more exoergic than HCl + O(^3P). Thus, after H migrates to F, the HFS($\tilde{X}\,^1A'$) surface will cross the triplet surface before all of the exoergicity is released, i.e., considerable potential energy will be released as the HF separates from S(^3P). Thus, the dynamics are similar to HF elimination reactions on singlet surfaces.[25,34,35]

V. CONCLUSIONS

By adding a prereactor to the infrared chemiluminescence flow reactor, the ClO and SF radicals were generated and subsequently reacted with H atoms. The H + ClO rate constant was determined as $(7.7 \pm 1.9) \times 10^{-11}$ cm^3 s^{-1} with branching to OH + Cl favored by a factor of 4.5. The OH vibrational distribution was determined as P_0–P_3 = 15:22:38:25 with $\langle f_V \rangle = 0.45$ and that for the HCl channel as P_0–P_4 = 24:25:27:16:8 with $\langle f_V \rangle = 0.31$. The bulk of the reaction proceeds via the HOCl($\tilde{X}\,^1A'$) ground state surface; the OH product is formed by adiabatic dissociation and HCl is formed by a crossing from the $\tilde{X}\,^1A'$ to the $\tilde{a}\,^3A''$ surface late in the HClO exit channel. A small component from direct reaction on the HOCl($\tilde{a}\,^3A''$) triplet surface may also contribute to HCl formation. Based upon consideration of microscopic reversibility, the classic study[8] of the role of vibrational energy in the Cl + OH(v) reaction may need reinterpretation because the bulk of the reaction may not proceed by direct reaction on the triplet surface. The H + SF reaction also proceeds over the $\tilde{X}\,^1A'$ surface, but the thermochemistry precludes formation of SH + F. The HF + S(^3P) products seem to be favored over the HF + S(^1D) products. The HF(v) rotational distributions are quite extended and estimates for the nascent rotational distributions were made; the energy partitioning pattern is $\langle f_V \rangle = 0.20$, $\langle f_R \rangle \sim 0.22$, and $\langle f_T \rangle \sim 0.6$. The rate constant for H + SF was not determined because [SF] was not controlled, but a value similar to that for H + ClO is likely. The H + ClO and H + SF reactions are good candidates for further study regarding the influence of switches between potential energy surface in the exit channel and reaction dynamics.[36]

ACKNOWLEDGMENTS

This work was supported by the National Science Foundation (86-01599). We thank Mr. Arunan for assistance with preparation of some figures.

[1]S. J. Wategaonkar and D. W. Setser, J. Chem. Phys. **90**, 251 (1988).
[2]J. A. Coxon, W. E. Jones and E. G. Skolnick, Can. J. Phys. **54**, 1043 (1976).
[3]M. W. Chase, Jr., C. A. Davies, J. R. Downey, Jr., D. J. Frurip, R. A. McDonald, and A. N. Syverud, J. Phys. Chem. Ref. Data **14**, Suppl. 1 (1985).
[4]P. P. Bemand, M. A. A. Clyne, and R. T. Watson, J. Chem. Soc. Faraday Trans. 1 **69**, 1356 (1973).
[5]M. A. A. Clyne, D. J. McKinney, and R. T. Watson, J. Chem. Soc. Faraday Trans. 1 **71**, 322 (1975).
[6]J. Brunning and M. A. A. Clyne, Faraday Trans. 2 **80**, 1001 (1984).
[7](a) P. A. G. O'Hare and A. C. Wahl, J. Chem. Phys. **54**, 3770 (1971); (b) M. C. R. Symons, in *Free Radicals in Inorganic Chemistry*, edited by R. F. Gould (American Chemical Society, Washington, D.C., 1962).
[8]B. A. Blackwell, J. C. Polanyi, and J. J. Sloan, Chem. Phys. **24**, 25 (1977).
[9]E. J. Kruss, B. I. Niefer, and J. J. Sloan, J. Chem. Phys. **88**, 985 (1988).
[10]P. H. Wine, J. R. Wells, and A. R. Ravishankara, J. Chem. Phys. **84**, 1349 (1986).
[11]A. C. Luntz, J. Chem. Phys. **73**, 5393 (1980).
[12]R. L. Jaffe and S. R. Langhoff, J. Chem. Phys. **68**, 638 (1978).
[13](a) D. J. Rakestraw, K. G. McKendrick, and R. N. Zare, J. Chem. Phys. **87**, 7341 (1987); (b) K. G. McKendrick, D. J. Rakestraw, and R. N. Zare, J. Chem. Soc. Faraday Discuss. **84**, 39 (1987).
[14]P. J. Bruna, G. Hirsch, S. D. Peyerimhoff, and R. J. Buenker, Can. J. Chem. **57**, 1839 (1979).
[15]R. Schinke, J. Chem. Phys. **80**, 5510 (1984).
[16]a. D. L. Baulch, R. A. Cox, P. J. Critzen, R. F. Hampson, Jr., J. A. Kerr, J. Troe, and R. T. Watson. J. Phys. Chem. Ref. Data **11**, 327 (1982); (b) G. Poulet, G. Laverdet, and G. LeBras, J. Phys. Chem. **90**, 159 (1986).
[17]B. S. Agrawalla and D. W. Setser, J. Phys. Chem. **90**, 2450 (1986).
[18]S. R. Langhoff, H. J. Werner and P. Rosmus, J. Mol. Spectrosc. **118**, 507 (1986).
[19]D. Oba, J. Ogilvie and D. W. Setser, J. Quant. Spectrosc. Radiat. Transfer (to be published).
[20]J. Habdas, S. J. Wategaonkar, and D. W. Setser, J. Phys. Chem. **92**, 451 (1987).
[21]K. R. Ryan and I. C. Plumb, Plasma Chem. Plasma Processes **4**, 141 (1984).
[22]H. W. Chang, D. W. Setser, and M. J. Perona, J. Phys. Chem. **75**, 2070 (1971).
[23]S. J. Wategaonkar, E. Arunan, and D. W. Setser (to be published).
[24](a)D. Klenerman and I. W. M. Smith, J. Chem. Soc. Faraday Trans. 2 **84**, 243 (1987); (b) J. C. Polanyi and K. B. Woodall, J. Chem. Phys. **57**, 1574 (1972).
[25]M. A. Wickramaaratchi, S. J. Wategaonkar, K. Tamagake, and D. W. Setser (to be published).
[26](a) J. P. Sung and D. W. Setser, Chem. Phys. Lett. **58**, 98 (1978); (b) R. J. Malins and D. W. Setser, J. Chem. Phys. **73**, 5666 (1980). After publication of this work, there was some concern that the SF_4 sample could have contained some SOF_2. However, direct tests of the H + SOF_2 reaction showed that the HF associated with H + SF_4 could not have been a consequence of SOF_2 impurity.
[27]S. Wategaonkar and D. W. Setser, J. Chem. Phys. **86**, 4477 (1987).
[28]M. A. Wickramaaratchi, D. W. Setser, B. Hildebrandt, B. Korbitzer, and H. Heydtmann, Chem. Phys. **84**, 105 (1984).
[29](a) J. C. Polanyi, J. L. Schreiber, and W. J. Skrlac, J. Chem. Soc. Faraday Discuss. **67**, 66 (1979); (b) A. M. G. Ding, L. J. Kirsch, D. S. Perry, J. C. Polanyi, and J. L. Schreiber, *ibid.* **55**, 252 (1973).
[30](a) C. B. Cleaveland, G. M. Jursich, M. Trolier, and J. R. Wiesenfeld, J. Chem. Phys. **86**, 3253 (1987); (b) P. M. Aker and J. J. Sloan, J. Chem. Phys. **85**, 1412 (1986); (c) Y. Huang, Y. Gu, C. Liu, X. Yang, and Y. Tao, Chem. Phys. Lett. **127**, 432 (1986); (d) J. E. Butler, G. M. Jurisch, I. A. Watson, and J. R. Wisenfeld, J. Chem. Phys. **84**, 536 (1986).
[31](a) P. J. Kuntz, B. I. Niefer, and J. J. Sloan, J. Chem. Phys. **88**, 3629 (1988); (b) R. Schinke and W. A. Lester, Jr., *ibid.* **70**, 4893 (1979); **72**, 3754 (1980); (c) S. W. Ransome and J. W. Wright, *ibid.* **77**, 6346 (1982); (d) P. A. Whitlock, J. T. Muckerman, and E. R. Fischer, J. Chem. Phys. **76**, 4468 (1982); (e) P. A. Elofson, K. Rynefors. and L. Holmlid, *ibid.* **100**, 39 (1985); (f) K. Rynefors, P. A. Elofson, and L. Holmid, *ibid.* **100**, 53 (1985).
[32]K. P. Huber and G. Herzberg, *Molecular Spectra and Molecular Structure, Vol IV* (Van Nostrand, New York, 1979).
[33]J. J. Sloan, D. G. Watson, J. M. Williamson, and J. S. Wright, J. Chem. Phys. **95**, 1190 (1981).
[34](a) E. Zamir and R. D. Levine, Chem. Phys. **52**, 253 (1980); (b) C. R. Quick, Jr. and C. Wittig, J. Chem. Phys. **72**, 1694 (1980); (c) D. J. Donaldson, D. G. Watson, and J. J. Sloan, Chem Phys. **68**, 96 (1982); (d) T. R. Fletcher and S. R. Leone, J. Chem. Phys. **88**, 4720 (1988).
[35]J. Malins and D. W. Setser, J. Phys. Chem. **85**, 1342 (1981).
[36]H. R. Mayne and J. C. Polanyi, J. Chem. Phys. **82**, 170 (1985).